Dynamics and Spectroscopy of Hydrogen Atoms on Pd{111}

Luis C. Fernández-Torres,[‡] E. Charles H. Sykes,[§] Sanjini U. Nanayakkara,[†] and Paul S. Weiss*,[†]

Departments of Chemistry and Physics, 104 Davey Laboratory, The Pennsylvania State University, University Park, Pennsylvania 16802-6300

Received: October 11, 2005; In Final Form: December 5, 2005

Chemisorption of hydrogen on Pd{111} is a relatively simple, yet important surface chemical process. By using low-temperature scanning tunneling microscopy, tip-induced motion of adsorbed atomic hydrogen at 4 K has been observed at low coverage. The motion has been ascribed to excitation of vibrational modes that decay into translational modes; vibrational spectroscopy via inelastic electron tunneling corroborates this assignment, and the barrier to hydrogen atom motion has been determined. At higher coverages, tip-induced motion of vacancies in the hydrogen overlayer is observed, and the associated barrier has also been determined.

1. Introduction

The interaction of hydrogen with transition metal surfaces is of paramount importance to the fundamental understanding of catalytic processes. Chemisorption of molecular hydrogen and its subsequent dissociation on transition metal surfaces is one of the simplest, yet most important processes for many industrially relevant catalytic reactions.[1] This interaction is also key to understanding metal embrittlement,[2] hydrogen separation,[3,4] hydrogen storage,[5] and emerging fuel cell technologies.[6,7] The interaction of hydrogen with Pd has been studied extensively both experimentally and theoretically.[8−16] Pd has the ability both to *adsorb* and to *absorb* hydrogen atoms. The adsorption of hydrogen on Pd surfaces has been characterized experimentally with several surface science techniques, including scanning tunneling microscopy (STM),[17,18] low-energy electron diffraction (LEED),[11,19] high-resolution electron energy loss spectroscopy,[10,19−22] temperature-programmed desorption (TPD),[11,12,19−23] and helium[22,24] and neutron[25,26] scattering. Results from those experimental techniques have provided valuable information on the H−Pd system, such as adsorption and desorption energies, surface vibrational features, overlayer structures, bulk diffusion barriers, and preferred adsorption sites.

Theoretical work on the H−Pd system has attempted to explain the observed surface experimental results.[9,14−16,27−29] By using various levels of theory, these studies have been able to explain correctly and to predict preferred adsorption sites, surface vibrational features, and overlayer structures. However, theoretical work has also predicted phenomena that have not been observed experimentally, such as Pd surface relaxations. Even though there is not complete agreement on the magnitude of the calculated values, there is consistency in the literature between the observed and predicted trends for the H−Pd system, such as preferred adsorption sites and overlayer structures.

Scanning tunneling microscopy is a powerful technique that allows the study of adsorbates at the atomic scale. It is the only technique that can probe the interactions of individual hydrogen atoms and hydrogen molecules with transition metal surfaces.[30−32] Additionally, scanning tunneling spectroscopy (STS), specifically inelastic electron-tunneling spectroscopy (IETS), provides atom-specific vibrational information that can be utilized to characterize the adsorbate−surface interaction.[32−34] The interaction of hydrogen with Pd{111} has been the subject of a recent STM investigation. Salmeron and co-workers determined the preferred adsorption site of hydrogen atoms on Pd{111}, overlayer structures, and diffusion barriers for individual hydrogen atoms and hydrogen overlayer vacancies on the Pd{111} surface.[17,18] Their pioneering investigation has helped visualize many interactions of hydrogen with Pd, while at the same time provided experimental evidence for and against some of the theoretical predictions for the H−Pd system. However, Salmeron and co-workers' work was limited by thermally induced effects, such as hydrogen surface diffusion.[17] More recently, we have demonstrated the manipulation of H atoms *under* the Pd{111} surface via inelastic excitation.[31]

In this paper, a scanning tunneling microscopy and spectroscopy investigation of hydrogen on Pd{111} at 4 K is presented. Conducting the experiments at 4 K eliminates the aforementioned thermally induced effects in this system. At low hydrogen exposures, tip-induced motion of atomic hydrogen at 4 K has been observed. The motion has been ascribed to inelastic excitation via tunneling electrons, and the barrier to hydrogen atom motion has been determined. Inelastic electron-tunneling spectroscopy has been utilized to probe the vibrational modes of single hydrogen atoms on Pd{111}, and these modes have been related to barriers of motion. Higher exposures of hydrogen result in formation of two ordered overlayer structures, namely $(\sqrt{3} \times \sqrt{3})$-2H and (1×1)-H. Furthermore, STM-tip-induced vacancy motion has been monitored, and the barrier to motion has been determined.

2. Experimental Section

The experiments presented in this report have been conducted on a custom-built, low-temperature, ultrastable, ultrahigh vacuum (UHV) STM that has been described in detail elsewhere.[35] The STM is stable enough to keep the STM tip positioned over a

* Corresponding author. E-mail: stm@psu.edu. Telephone: +1-814-865-3693. Fax: +1-814-863-5516.

[†] Departments of Chemistry and Physics, 104 Davey Laboratory, The Pennsylvania State University.

[‡] Current address: Department of Chemistry, University of Puerto Rico at Cayey, Cayey, Puerto Rico.

[§] Current address: Department of Chemistry, Tufts University, Medford, Massachusetts.

10.1021/jp055815e CCC: $33.50 © 2006 American Chemical Society
Published on Web 03/18/2006

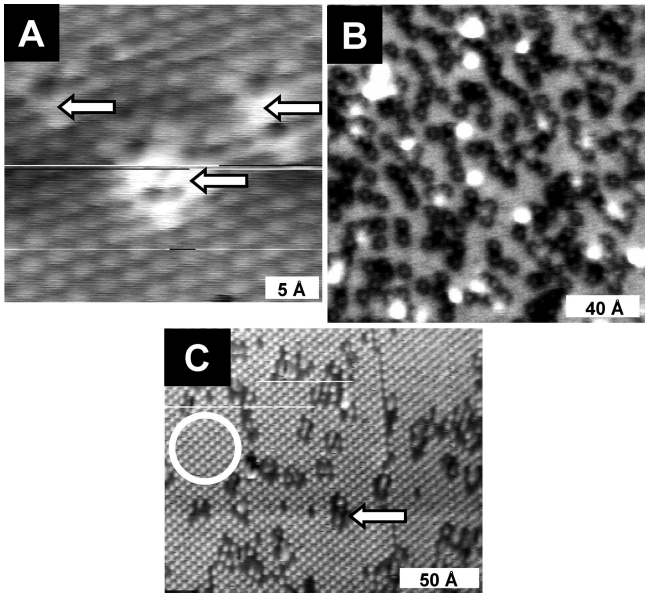

Figure 1. STM images of Pd{111} as a function of hydrogen coverage. (A) STM image of a 30 Å × 30 Å region of a clean Pd{111} surface. Subsurface impurities are observed and highlighted with left-pointing arrows. ($V_{sample} = +0.03$ V, $I_t = 150$ pA). (B) STM image of a 175 Å × 175 Å region for 0.1 ML of hydrogen. The apparent depressions are hydrogen atoms, the protrusions are subsurface impurities. ($V_{sample} = +0.10$ V, $I_t = 50$ pA). (C) STM image of a 200 Å × 178 Å region for 0.7 ML of hydrogen. The protrusions are hydrogen overlayer vacancies arranged in a ($\sqrt{3} \times \sqrt{3}$) structure, which corresponds to a ($\sqrt{3} \times \sqrt{3}$)-2H structure (circle). The topographically lower areas are (1 × 1)-H (left-pointing arrow). ($V_{sample} = +0.09$ V, $I_t = 100$ pA).

single atomic site for hours or days at a time. All STM topographic images have been recorded at 4 K in constant-current mode with a mechanically cut Pt/Ir (85:15%) tip. All biases in the STM images are referenced to the sample bias. Inelastic electron-tunneling spectroscopy has been acquired utilizing a lock-in amplifier (Stanford Research Systems, model SR830) to monitor the current's second harmonic (d^2I/dV^2) directly with an ac amplitude of 4 mV (rms) at 1000 Hz modulation. Time-lapse STM images consist of a series of topography images of the same area acquired over a period of 12 h. Acquisition of each image takes approximately 3 min. The time-lapse STM images presented here were acquired with sample biases of +0.07, +0.10, and +0.15 V, as indicated.

The single-crystal Pd{111} surface (MaTecK) was cleaned by repeated cycles of Ar^+ sputtering (1000 eV, $I_{sample} = 5\ \mu$A) at 873 K for 15 min, followed by oxygen treatment (873 K, 1.0×10^{-5} Torr O_2 backfill for 5 min), and annealing in a vacuum (1100 K for 10 min). Pd{111} cleanliness was assessed with STM. Hydrogen gas (Matheson, 99.95%) was dosed at room temperature on the Pd{111} surface by backfilling the UHV chamber to 2.0×10^{-8} Torr via a leak valve. The room-temperature chamber's base pressure was measured to be 2.0×10^{-10} Torr. The low-temperature chamber's base pressure is orders of magnitude lower due to cryopumping. Dosing at room temperature ensures the presence of adsorbed atomic hydrogen, as molecular hydrogen readily dissociates on Pd{111} at temperatures as low as 37 K.[18]

3. Results and Discussion

3.1. Adsorption of Hydrogen on Pd{111}. Figure 1 contains a series of images of atomic hydrogen adsorbed on Pd{111} as a function of coverage. A representative STM image of a "nominally clean" Pd{111} with atomic resolution (Figure 1A) shows the hexagonal arrangement of the Pd atoms and subsurface impurities (denoted with left-pointing arrows).[36] Subsurface impurities are ubiquitous in STM studies of Pd single crystals, and have been characterized by Salmeron and co-workers. Nonetheless, a constant low concentration (<0.01%) of these impurities (assigned as S, C, and O by Salmeron and co-workers)[36] can be obtained through cycles of sample treatments, producing a nominally clean Pd surface. The subsurface impurities that appear in Figure 1A as protrusions are ascribed to either C or O; these are difficult to discern from one another.[36] Salmeron and co-workers have also demonstrated that the potential effects on the adsorption of hydrogen on Pd{111} of these subsurface impurities can be largely excluded, as they did not observe subsurface impurity effects on hydrogen overlayer structures or diffusion.[17,36] We have recently produced and identified subsurface hydride species that do affect the hydrogen overlayer,[31] but those hydride species are not present here. Figure 1B displays a STM image recorded at ~0.1 ML coverage of hydrogen on Pd{111}. The hydrogen atoms are imaged as depressions with a bare metallic tip.[17] The protrusions are subsurface impurities. No ordered structures were observed; the hydrogen atoms arrange themselves in small clusters and chains with no particular order or preferred direction. Figure 1C shows an image of a ~0.7 ML coverage of hydrogen on Pd{111}. The protrusions are assigned as vacancies on a depressed background; this background corresponds to a ($\sqrt{3} \times \sqrt{3}$)-2H overlayer (circle).[17] The vacancies (sites not occupied by hydrogen atoms) are ordered in a ($\sqrt{3} \times \sqrt{3}$) pattern, with the two hydrogen atoms located at interstitial positions in this structure. The topographically lower areas observed in Figure 1C are (1 × 1)-H areas (left-pointing arrow). Previous experimental and theoretical studies have determined that the most stable adsorption site for hydrogen on Pd{111} is the 3-fold hollow site that is directly above a second-layer hollow site. This surface site is referred to as the face-centered cubic (fcc) site.[14,16,17] The images presented in Figure 1 do not show the adsorption site. Nevertheless, atomically resolved images of Pd{111} with adsorbed hydrogen atoms (not shown), and observation of these ordered structures, are consistent with a fcc adsorption site.[17,36]

3.2. Tip-Induced Motion of Hydrogen on Pd{111}. Motion of hydrogen atoms adsorbed on Pd{111} has been observed for 0.1 ML coverage. Scanning tunneling microscopy images were acquired at 4 K; therefore, thermally induced motion can be ruled out. Furthermore, motion of hydrogen atoms on Pd{111} has only been observed at specific sample biases. Time-lapse STM images (Supporting Information), acquired at different voltages, show no motion at 0.07 V, some motion at 0.10 V, and more rapid motion at 0.15 V. Exactly the same trend has been observed at the corresponding negative sample biases. Acquisition of additional time-lapse STM images at different sample biases yields an onset for tip-induced hydrogen atom motion of 0.10 V at both bias polarities. Salmeron and co-workers also studied the diffusion of hydrogen on Pd{111} and used thermally induced hopping rates to determine that the activation barrier for hydrogen diffusion is 0.09 eV[17] from measurements at 37 K. Theoretical studies of the activation barrier for hydrogen diffusion on Pd{111}[14,16,37] predict values from 0.135 to 0.17 eV, which are higher than the value determined in both the previous and the present work. Diffusion of subsurface impurities does not occur in the voltage range studied. Salmeron and co-workers observed diffusion of sub-

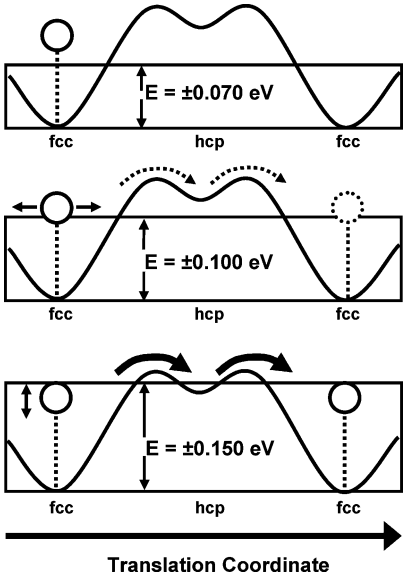

Figure 2. Schematic depicting the tip-induced motion of hydrogen atoms on Pd{111} along the translation coordinate. The energies included in the figure correspond to the energies from the hydrogen motion time-lapse STM images. The potential energy pathway comes from values derived in ref 14.

surface impurities in Pd{111} at 210 K, and determined diffusion barriers for these impurities to be on the order of 1 eV.[36]

The schematic presented in Figure 2 illustrates the mechanism for atomic hydrogen motion on the Pd{111} surface deduced from observations from time-lapse STM images and theoretically predicted potential energies. The schematic shows the motion of a hydrogen atom along a fcc−hcp−fcc path, passing two Pd atoms via a bridge site. The hexagonal close-packed (hcp) site refers to the 3-fold hollow surface site that is directly above a second-layer Pd atom. Theoretical studies predict that this path is the lowest energy path for hydrogen surface motion,[14] and the shape of the potential energy profile in Figure 2 corresponds to these theoretical results. When excited by tunneling electrons at 0.07 V (at either bias polarity), the hydrogen atoms do not have sufficient energy to overcome the barrier to motion. With tunneling electrons at 0.10 V, the hydrogen atoms barely possess sufficient energy to overcome the barrier to motion.[16,27] With tunneling electrons at 0.15 V, the barrier to motion is easily overcome, and hydrogen atom motion on Pd{111} at 4 K occurs readily. Sautet and co-workers predicted a barrier to hydrogen motion of 0.150 eV along the path illustrated,[14] which is in rough agreement with the time-lapse STM images and the schematic in Figure 2. However, the onset for hydrogen motion on the Pd{111} surface has been determined as 0.10 V from the time-lapse STM images. The possibility of a path with a lower barrier to motion cannot be ruled out because some motion is observed at ±0.10 V sample bias.[16,27] This point is addressed below with IETS in Section 3.3.

Tip-induced motion of hydrogen atoms on Pd{111} is shown in Figure 3. This figure presents a region extracted from an STM image, where the hydrogen atoms "jump" from one adsorption site to another along the scanning direction. The adjacent schematic illustrates how a hydrogen atom jumps from a fcc site to another fcc site along the scanning direction and is imaged multiple times. The arrangement of the Pd atoms in the schematic reflects the lattice orientation, determined from atomically resolved images of the same region (not shown). The hydrogen atom moves from fcc site to fcc site because scanning

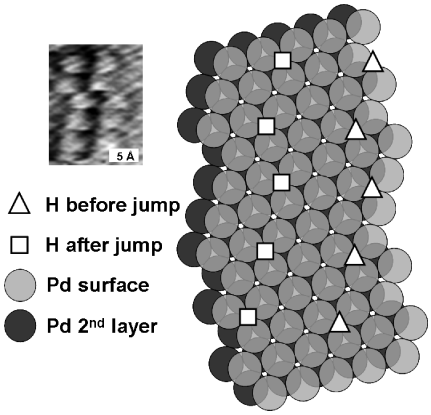

Figure 3. Small region (11 Å × 16 Å) extracted from an STM image ($V_{sample} = -0.15$ V, $I_t = 150$ pA), where hydrogen atoms "hop" from fcc to fcc sites. The schematic on the right illustrates the positions before and after the jumps. The length of the jump in the scanning direction ([2 $\bar{3}$ 1] with respect to the Pd lattice) corresponds to the Pd interatomic distance (2.75 Å) × $2\sqrt{2}$.

at −0.15 V sample bias provides sufficient energy to overcome the barrier to motion.

3.3. Tunneling Spectroscopy of Hydrogen on Pd{111}. To understand the observed barriers to motion, local vibrational spectroscopy via inelastic electron-tunneling spectroscopy (IETS)[30,33,34,38] has been performed on both bare Pd{111} and hydrogen on Pd{111}. Figure 4A displays the IETS spectrum for bare Pd{111}, which contains features only at ±0.02 V. Experimentally, a Pd surface phonon feature has been detected with helium scattering and measured in the range of 0.020−0.030 eV.[39] Molecular dynamics simulations have predicted a peak at 0.023 eV resulting from a Pd phonon motion.[40] The feature in Figure 4A agrees well with these values, and has been assigned as a Pd phonon mode. This feature cannot be attributed to Pd hydride because Pd hydride vibrations are more energetic (0.056 and 0.096 eV).[22] This spectrum has been utilized as the background signal for IETS of hydrogen on Pd{111}, which is shown in Figure 4B. Difficulties arose during the acquisition of IETS spectra of individual hydrogen atoms at low coverage because the hydrogen atoms repeatedly moved away from the tunneling junction during the measurements. Therefore, the hydrogen on Pd{111} IETS spectra have been acquired on hydrogen atoms in a (1 × 1)-H structure, as the tighter packing prevents hydrogen motion away from the tunneling junction. High-resolution electron energy loss spectroscopy studies of different hydrogen exposures adsorbed on Pd{111} at liquid nitrogen temperatures have shown minimal effects due to differences in hydrogen coverage.[10,22] In addition to the Pd phonon feature, the IETS spectra of hydrogen on Pd{111} contains three features for each bias polarity, centered at ±0.08 V (triangle arrow), ±0.15 V (diamond arrow), and ±0.20 V (ellipse arrow). High-resolution electron energy loss spectroscopy studies have determined two vibrational modes for atomic hydrogen on Pd{111}: a mode parallel to the surface (rocking motion) at 0.096 eV, and a mode perpendicular to the surface (stretch) at 0.124 eV.[10,22] Accordingly, the features in the IETS spectra located at ±0.08 and ±0.15 V have been assigned to the parallel mode and perpendicular mode, respectively. The feature at ±0.20 V remains unassigned. We note that IETS spectra were always acquired with a STM probe tip that resulted in image contrast typical for a bare Pt/Ir tip[17] before and after acquiring spectra so as to eliminate the possibility that spectra features were the result of adsorbates on the tip. The positions of the peaks and the dips in the IETS spectra with

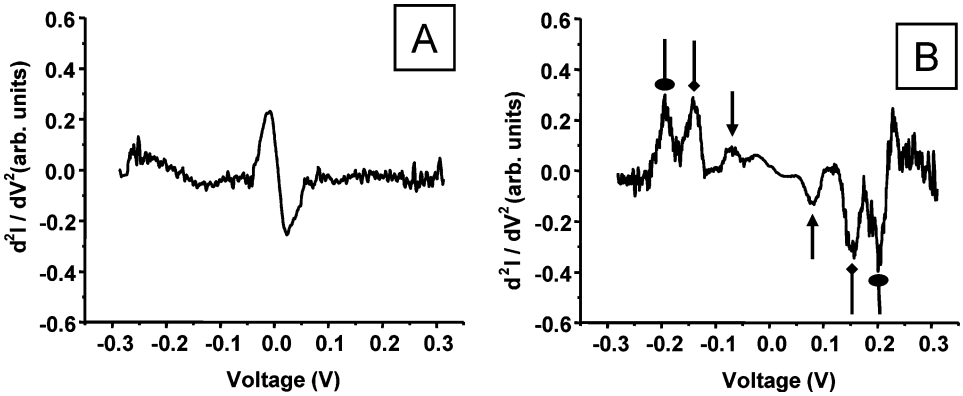

Figure 4. Inelastic electron-tunneling spectra of (A) clean Pd{111} and (B) hydrogen on Pd{111}. The markers in (B) illustrate the symmetry of the features with respect to 0 V bias.

respect to bias polarity suggest a complex relationship between the vibrational excitations and electronic resonances, producing a decrease in tunneling conductance; this effect has been observed previously.[38]

The hydrogen on Pd{111} IETS spectra provide insight into the magnitude of the hydrogen motion barrier and the mechanism by which it occurs. From the time-lapse STM images, the onset for tip-induced hydrogen motion has been determined to be 0.10 V. According to the IETS spectrum in Figure 4B, at 0.10 V, the parallel mode is excited, but it does not possess enough energy to couple efficiently to atomic translation. As the excitation energy increases, the perpendicular mode becomes excited beyond 0.14 V and couples more efficiently to atomic translation. This mechanism, whereby tunneling electrons excite a vibrational mode whose energy is subsequently dissipated through translation, is referred to as inelastic tunneling-induced motion.[41−43] This adsorbate motion mechanism has been observed previously for mode-selective diffusion of NH_3 on Cu{100},[42] and lateral hopping of CO molecules on Pd{110}.[43] In the case of hydrogen atom motion on the Pd{111} surface at 4 K, tunneling electrons excite the perpendicular (stretch) vibrational mode. The energy of the perpendicular mode is then dissipated through coupling between the perpendicular mode and translation, and hydrogen atom motion is readily observed.

3.4. Tip-Induced Vacancy Motion. Previously, Salmeron and co-workers investigated the diffusion of vacancies in the (1×1)-H overlayer on Pd{111}.[17] Those investigations used vacancy hopping rates at 65 K to estimate a vacancy diffusion barrier of 0.21 eV. Vacancy diffusion was ascribed as thermally induced. In the present study, time-lapse STM images at 4 K yield 0.22 V as the vacancy motion onset. Thermally induced motion cannot adequately describe the observed vacancy motion onset on Pd{111} at 4 K. Vacancy motion has been observed only at energies beyond the IETS features. The value for the vacancy motion onset (0.22 V) is close to the experimentally determined bulk diffusion barrier for hydrogen in Pd (0.23 eV),[8,12] suggesting that hydrogen motion into (or out of) the Pd crystal enables vacancy motion. Theoretical calculations suggest that barriers to hydrogen atom diffusion in bulk Pd are predominantly independent of the diffusion path,[15] allowing for essentially isotropic hydrogen atom mobility below the surface. This observation also suggests hydrogen atom mobility into the crystal could be tip-induced through the excitation of vibrational modes.

4. Conclusions

The dynamics and spectroscopy of hydrogen adsorbed on Pd{111} have been investigated at 4 K. At low hydrogen coverage, no ordered structures were discerned from STM images, and tip-induced motion of atomic hydrogen at 4 K has been observed. The motion has been ascribed to inelastic excitation by tunneling electrons; IETS corroborates this assignment, and the barrier to hydrogen atom motion has been determined to be 0.10 V. Inelastic electron-tunneling spectroscopy features associated with a parallel vibrational mode (0.08 V), and a perpendicular vibrational mode (0.15 V) have been determined and observed at both bias polarities. Scanning tunneling microscope tip-induced vacancy motion has been observed, and the barrier to vacancy motion has been determined to be 0.22 V.

Acknowledgment. The authors gratefully acknowledge the following funding agencies for providing financial support for this investigation: Air Force Office of Scientific Research, Army Research Office, Defense Advanced Research Projects Agency, National Science Foundation, and Office of Naval Research. The authors wish to thank Dr. Patrick Han and Dr. Daniel J. Fuchs for their help with the time-lapse STM images and the Pd{111} sample.

Supporting Information Available: Time-lapse STM images acquired at sample biases of 0.07, 0.10, and 0.15 V and tunneling currents of 50 pA. This material is available free of charge via the Internet at http://pubs.acs.org.

References and Notes

(1) *Hydrogen Effects in Catalysis. Fundamentals and Practical Applications*; Paal, Z., Menon, P. G., Eds.; Dekker: New York, 1988; Vol. 31, p 753.

(2) *Hydrogen Embrittlement. Prevention and Control*; Raymond, L., Ed.; American Society for Testing and Materials: Philadelphia, 1988; p 434.

(3) Moss, T. S.; Peachey, N. M.; Snow, R. C.; Dye, R. C. *Int. J. Hydrogen Energy* **1998**, *23*, 99.

(4) Tosti, S.; Bettinali, L.; Violante, V. *Internat. J. Hydrogen Energy* **2000**, *25*, 319.

(5) *Hydrogen Storage Materials*; Barnes, R. G., Ed.; Trans Tech Publications: Aedermannsdorf, Switzerland, 1988; p 350.

(6) Wieckowski, A.; Kim, H.; Rice, C.; Waszczuk, P. *Proc. Electrochem. Soc.* **2001**, *2000−20*, 91.

(7) Choudhary, T. V.; Aksoylu, E.; Goodman, D. W. *Catal. Rev.—Sci. Eng.* **2003**, *45*, 151.

(8) *Hydrogen in Metals I*; Völkl, J., Alefeld, G., Eds.; Springer: Berlin, 1978; Vol. 28, p 321.

(9) Eberhardt, W.; Louie, S. G.; Plummer, E. W. *Phys. Rev. B* **1983**, *28*, 465.

(10) Conrad, H.; Kordesch, M. E.; Scala, R.; Stenzel, W. *J. Electron Spectrosc. Relat. Phenom.* **1986**, *38*, 289.

(11) Behm, R. J.; Penka, V.; Cattania, M.-G.; Christmann, K.; Ertl, G. *J. Chem. Phys.* **1983**, *78*, 7486.

(12) Kay, B. D.; Peden, C. H. F.; Goodman, D. W. *Phys. Rev. B* **1986**, *34*, 817.
(13) Rieder, K.-H.; Baumberger, M.; Stocker, W. *Phys. Rev. Lett.* **1983**, *51*, 1799.
(14) Paul, J.-F.; Sautet, P. *Phys. Rev. B* **1996**, *53*, 8015.
(15) Löber, R.; Hennig, D. *Phys. Rev. B* **1997**, *55*, 4761.
(16) Løvvik, O. M.; Olsen, R. A. *Phys. Rev. B* **1998**, *58*, 10890.
(17) Mitsui, T.; Rose, M. K.; Fomin, E.; Ogletree, D. F.; Salmeron, M. *Surf. Sci.* **2003**, *540*, 5.
(18) Mitsui, T.; Rose, M. K.; Fomin, E.; Ogletree, D. F.; Salmeron, M. *Nature* **2003**, *422*, 705.
(19) Muschiol, U.; Schmidt, P. K.; Christmann, K. *Surf. Sci.* **1998**, *395*, 182.
(20) Okuyama, H.; Siga, W.; Takagi, N.; Nishijima, M.; Aruga, T. *Surf. Sci.* **1998**, *401*, 344.
(21) Okuyama, H.; Nakagawa, T.; Siga, W.; Takagi, N.; Nishijima, M.; Aruga, T. *J. Phys. Chem. B* **1999**, *103*, 7876.
(22) Farías, D.; Schilbe, P.; Patting, M.; Rieder, K.-H. *J. Chem. Phys.* **1999**, *110*, 559.
(23) Cabrera, A. L.; Morales, E.; Armor, J. N. *J. Mater. Res.* **1995**, *10*, 779.
(24) Hsu, C.-H.; Larson, B. E.; El-Batanouny, M.; Willis, C. R.; Martini, K. M. *Phys. Rev. Lett.* **1991**, *66*, 3164.
(25) Kemali, M.; Totolici, J. E.; Ross, D. K.; Morrison, I. *Phys. Rev. Lett.* **2000**, *84*, 1531.
(26) Nicol, J. M.; Rush, J. J.; Kelley, R. D. *Phys. Rev. B* **1987**, *36*, 9315.
(27) Dong, W.; Ledentu, V.; Sautet, P.; Eichler, A.; Hafner, J. *Surf. Sci.* **1998**, *411*, 123.
(28) Nobuhara, K.; Kasai, H.; Nakanishi, H.; Okiji, A. *J. Appl. Phys.* **2002**, *92*, 5704.
(29) Kang, B.-S.; Sohn, K.-S. *Physica B* **1996**, *217*, 160.
(30) Lauhon, L. J.; Ho, W. *Phys. Rev. Lett.* **2000**, *85*, 4566.
(31) Sykes, E. C. H.; Fernández-Torres, L. C.; Nanayakkara, S. U.; Mantooth, B. A.; Nevin, R. M.; Weiss, P. S. *Proc. Natl. Acad. Sci. U.S.A.* **2005**, *102*, 17907.
(32) Gupta, J. A.; Lutz, C. P.; Heinrich, A. J.; Eigler, D. M. *Phys. Rev. B* **2005**, *71*, 115416.
(33) Pascual, J. I.; Jackiw, J. J.; Song, Z.; Weiss, P. S.; Conrad, H.; Rust, H. P. *Phys. Rev. Lett.* **2001**, *86*, 1050.
(34) Stipe, B. C.; Rezaei, M. A.; Ho, W. *Science* **1998**, *280*, 1732.
(35) Ferris, J. H.; Kushmerick, J. G.; Johnson, J. A.; Youngquist, M. G. Y.; Kessinger, R. B.; Kingsbury, H. F.; Weiss, P. S. *Rev. Sci. Instrum.* **1998**, *69*, 2691.
(36) Rose, M. K.; Borg, A.; Mitsui, T.; Ogletree, D. F.; Salmeron, M. *J. Chem. Phys.* **2001**, *115*, 10927.
(37) Watson, G. W.; Wells, R. P. K.; Willock, D. J.; Hutchings, G. J. *J. Phys. Chem. B* **2001**, *105*, 4889.
(38) Hahn, J. R.; Lee, H. J.; Ho, W. *Phys. Rev. Lett.* **2000**, *85*, 1914.
(39) Hsu, C.-H.; El-Batanouny, M.; Martini, K. M. *J. Electron Spectrosc. Relat. Phenom.* **1990**, *54/55*, 353.
(40) Lynch, D. L.; Rick, S. W.; Gomez, M. A.; Spath, B. W.; Doll, J. D.; Pratt, L. R. *J. Chem. Phys.* **1992**, *97*, 5177.
(41) Komeda, T.; Kim, Y.; Kawai, M.; Persson, B. N. J.; Ueba, H. *Science* **2002**, *295*, 2055.
(42) Pascual, J. I.; Lorente, N.; Song, Z.; Conrad, H.; Rust, H.-P. *Nature* **2003**, *423*, 525.
(43) Komeda, T.; Kim, Y.; Kawai, M. *Surf. Sci.* **2002**, *502*−*503*, 12.